Romanian Journal of Petroleum & Gas Technology
Vol. V (LXXVI) • No. 1/2024

INTERPRETATION OF MAGNETIC AND GRAVIMETRIC SIGNATURES IN RELATION TO GEOLOGICAL STRUCTURES OF PETROLEUM INTEREST IN THE WESTERN PART OF THE CENTRAL BASIN OF THE DR CONGO

Joel Etshekodi Lohadje [1, 2]

Marlin Agolo Monza [2]

[1] Geology Survey-DRC (SGN-C), Kinshasa, DR Congo,
[2] Faculty of Oil, Gas and Renewable Energies, University of Kinshasa, DR Congo,
email (corresponding author): joellohadje@gmail.com

DOI: 10.51865/JPGT.2024.01.03

ABSTRACT

The Cuvette Centrale is a sedimentary basin stretching from the Democratic Republic of the Congo to the Republic of Congo, Gabon and Angola. The existence of hydrocarbons in this large basin is demonstrated by the presence of indications on the DR Congo side and by the discovery of hydrocarbons by the Ngoki well (Republic of Congo) diagonally across the Lokoro sub-basin (DR Congo). In view of this evidence, the four boreholes drilled in the DR Congo's Cuvette Centrale have not reported the presence of hydrocarbons. With this in mind, this study reinterprets the geophysical data (magnetism and gravimetry) to highlight geological structures of petroleum interest. After processing and interpretation, we understand that the region contains interesting structures linked to hydrocarbon trapping. These include anticlines and faults. We discovered that there is a close relationship between the geological structures of these two countries (DR Congo and R Congo). They are all made up of the same geological structures separated by two major strike-slip faults crossed by the Congo River (NE-SW direction). These are the Dextre Fault, which displaces the compartments on the DR Congo side in a SW-NE direction, and the Senestre Fault, which runs NE-SW.

Keywords: fault, dextre, senestre, geological structures, anomaly, Congo Basin

INTRODUCTION

Petroleum exploration work in the Cuvette Centrale was carried out by several foreign companies and organizations, including the Brussels laboratories of Tervuren, CGG and the Belgian firm Remina. Carried out around the 1950s, this work consisted of geological, geochemical and geophysical methods, followed by their respective interpretations and sanctioned by stratigraphic and exploration drilling: Dekese and Samba, which were drilled on the shoal, then after seismic testing, which led to the new locations of two other boreholes, Mbandaka and Gilson, limited to the schistose limestone (down to the salt) [1]. None of these four boreholes revealed a liter of hydrocarbons on the surface. In addition, an oil well drilled on the Republic of Congo side revealed the presence of hydrocarbons in the Ngoki Block of the Cuvette Centrale [2]. The latter is diagonal to the Lokoro sub-basin of the DR Congo's Cuvette Centrale,

separated by the Congo River. (This gives us the motivation to study the western part of the Democratic Republic of Congo in order to determine the necessary geological structures linked to oil traps, as the presence of hydrocarbons has been reported diagonally to the DR Congo, precisely in the Republic of Congo. To do this, we are processing and interpreting gravity and magnetic data from the geophysical campaign undertaken by Remina to highlight interesting structures linked to the petroleum system. Data processing and interpretation were carried out using Oasis-Montaj software, and involved the application of filters to deduce interesting geological structures related to hydrocarbons.

GEOGRAPHICAL LOCATION OF THE STUDY AREA

Location

Our study area is located in the western part of the Democratic Republic of Congo, on the border with the Republic of Congo. It is bordered to the west by the Republic of Congo and the Congo River, to the east by the Province of Tshuapa, to the south by the Province of Mayi-Ndombe and to the north by the Territory of Bolamba and Basankusu. It is located between 15° and 20° East longitude and 1°N and 2°S latitude. As for the region's hydrography, the majestic Congo River flows through the area, as do a number of large rivers. Two large lakes, including Mayi-Ndombe Lake, are located in the province of Mayi-Ndombe, and to the north of the latter is a small lake located in the SW of the province of Equateur (Figure 1).

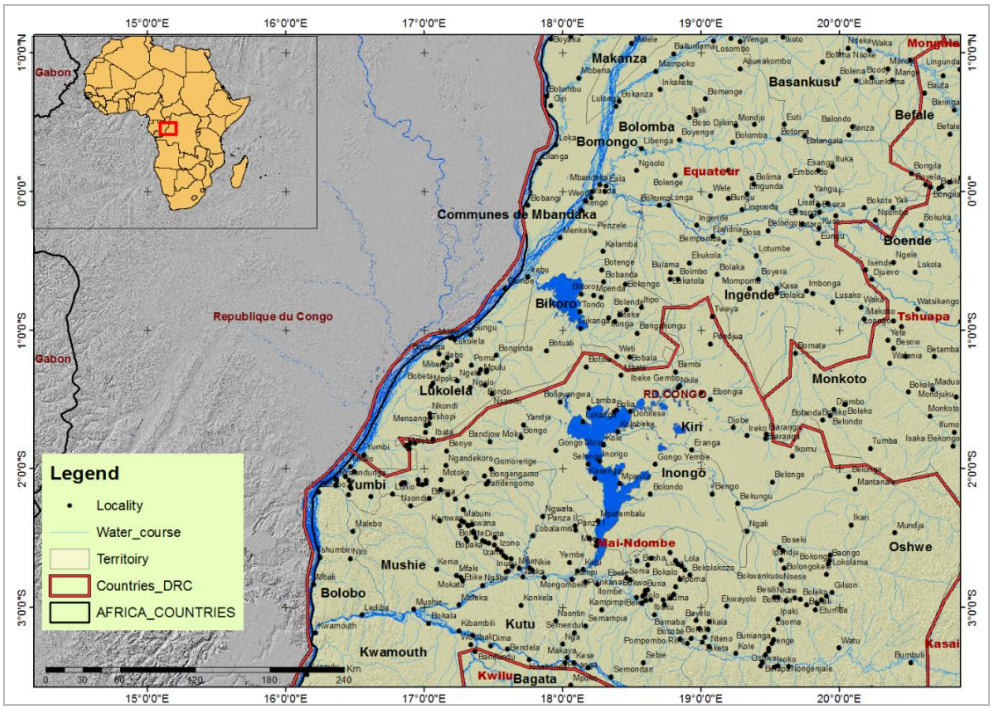

***Figure 1**. Location of the study area*

Topography

The topography of the region shows altitudes ranging from 200 to 700m. Our study area is a depression with altitudes below 300m. The peripheries of the area are dominated by high altitudes ranging from 500 to 700m. The low-lying areas correspond to the watercourse (Figure 2).

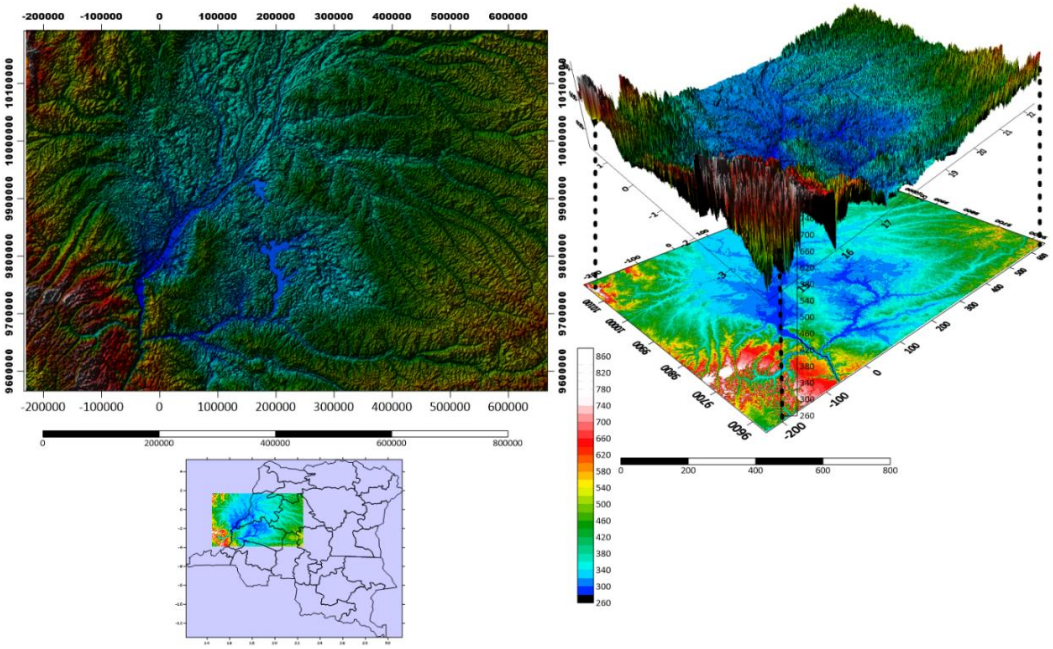

***Figure 2**. Topographical map of the study area*

GEOLOGICAL SETTING

Geology

Paleogene, Neogene and Miocene: The Neogene and Paleogene are the Cenozoic formations preceding the Quaternary, which is a recent geological formation. These formations are of the Phanerozoic type, i.e., the overlying formations above the basement or Precambrian. This cover (Phanerozoic) covers all geological time since the beginning of the Paleozoic (or Primary) era.

Neogene: this is the most recent part of the Tertiary era, covering the Miocene and Pliocene (with the exception of the Upper Pliocene). It contains series that are large, layered units, but do not coincide with those of classical geology, so these series have local names. In most cases, they have a characteristic paleontological content.

These series contain ochre sands, which are clay soils colored red by hematite (Fe_2O_3), iron combined with oxygen (red or blood ochre), yellow or brown by goethite, which gives yellow ochres (FeO-OH), or limonite, which uses clays as a colorant (iron hydroxides mixed with clays to give yellows). These sands and silts, generally ochre-colored and often bleached on the surface, are locally underlain by limonitic armour, sometimes accompanied by gravel, sometimes replaced by gravel, resting on a mid-Tertiary erosion surface up to 120 m thick.

Paleogene: polymorphous sandstone. Sandstones are terrigenous detrital sedimentary rocks (resulting from the erosion of land by water) at least 85% composed of more or less rounded quartz grains, from 1/16mm (62.5µm) to 2mm (arenite class). These rocks make up the bulk of many stratigraphic series, in regular or irregular beds, or in lenses. These rocks are whitish to light gray, or variously colored, depending on the nature of the cement, in red (iron oxides) or green (glauconites, etc.). Varieties are distinguished according to grain, nature of cement and/or presence of particular elements.

These series contain sands, soft sandstones and millstones ("polymorphic sandstones"): sandstones, limestones and silicified clay rocks (Figure 3). At the base, often conglomerate, sometimes with eolianized pebbles (wind-worn surface loaded with sand grains, generally satin-finish and pecked, locally laterite, resting on an erosion surface of late Cretaceous age. These series can be up to 80m thick. These ochre sand series and the polymorphous sandstone series, with the exception of the more recent sands, are frequently referred to as the "Kalahari system". They only outcrop in the southern half of the DRC.

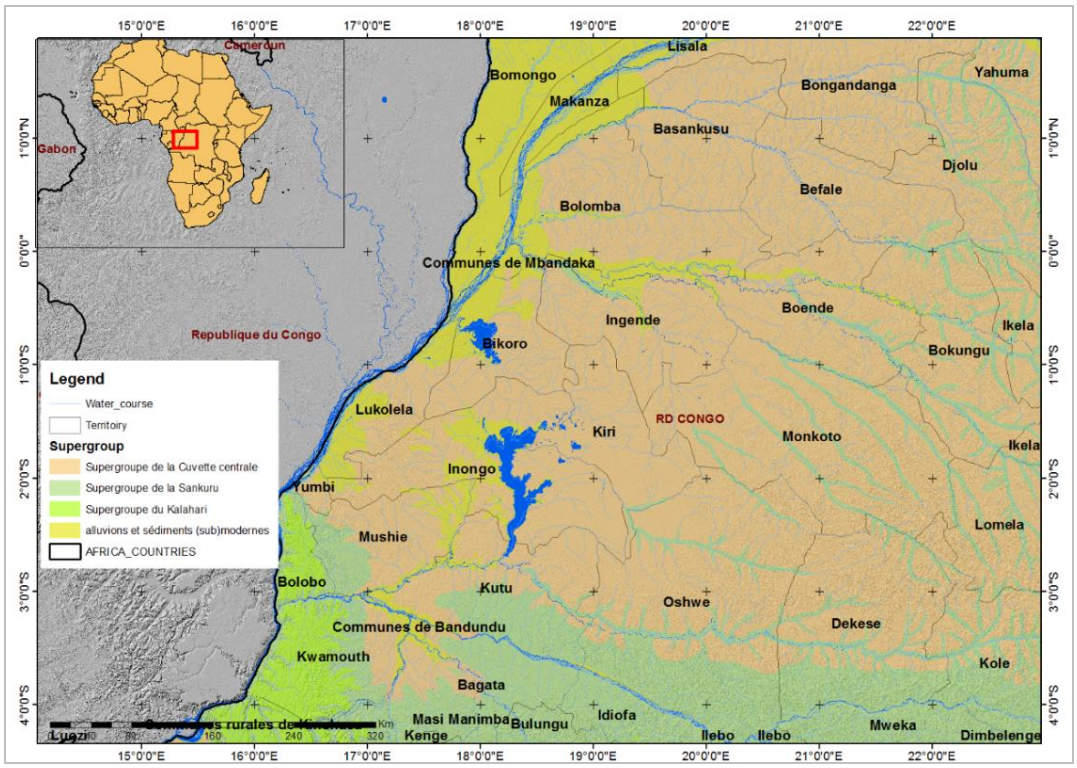

***Figure 3**. Geological map of the study area*

Pleistocene and Pliocene: The Pleistocene is the lower, most recent part of the Quaternary. The Pleistocene is the stratigraphic division at the end of the Tertiary Era.

Pleistocene: subaerial formations consisting of silts and superficial sands, eluvium and colluvium, reworking gravels, slope scree (horizons of rocky or ferruginous rubble).

Pliocene: ancient fossilized soils with induration horizons formed of ferruginous grit and shells (frequently lateritic), carbonate concretions. Other local formations include ossiferous breccias and/or breccias with prehistoric tools (guanos), the deposits of thermal springs (travertines).

Maestrichtian: this is the highest stage of the Cretaceous, and thus marks the end of the Secondary Era. It comprises dolomitic sandstone limestones, dolomitic shell limestones, dolomitic clay limestones, marls, calcodolomitic cement poudingues and quartz pebbles. These grey or yellow rocks are frequently phosphate-bearing. Estimated thickness: 125m.

The **Campanian and Santonian** are made up of dolomitic shell limestones, dolomitic sandstone limestones, marls, calcodolomitic sandstones, poudingues with carbonate

paste and quartz and quartzite pebbles, white, grey or yellow rocks. The thickness of the Campanian is estimated at 95 m, that of the Santonian at 405 m [3].

Stratigraphy

Sedimentation reflects structural evolution, resulting in the presence of several horsts and ditches [4] with a sedimentary fill of up to 12 km. The stratigraphy of the Cuvette Centrale (Figure 4) shows polymorphous sandstones and ochre sands of fluvial and eolian origin of Cenozoic age at the base. The Upper Paleozoic includes Carboniferous and Permian formations. From the Upper Proterozoic to the Paleozoic (Devonian), three groups have been identified: The Proterozoic age group, consisting of lagoonal marginal marine sediments. The Cambrian age group, with deposits of alluvial origin (Bobwamboli arkoses) and Mamungi and Kolé shales of deltaic facies. The Ordovician, Silurian and Devonian age group containing Galamboge quartzites (marine dunes), Alolo shales (fluvial) and Banalia arkoses (deltaic). Knowledge of the stratigraphy of the Cuvette Centrale basin also depends on progressive geological exploration [5].

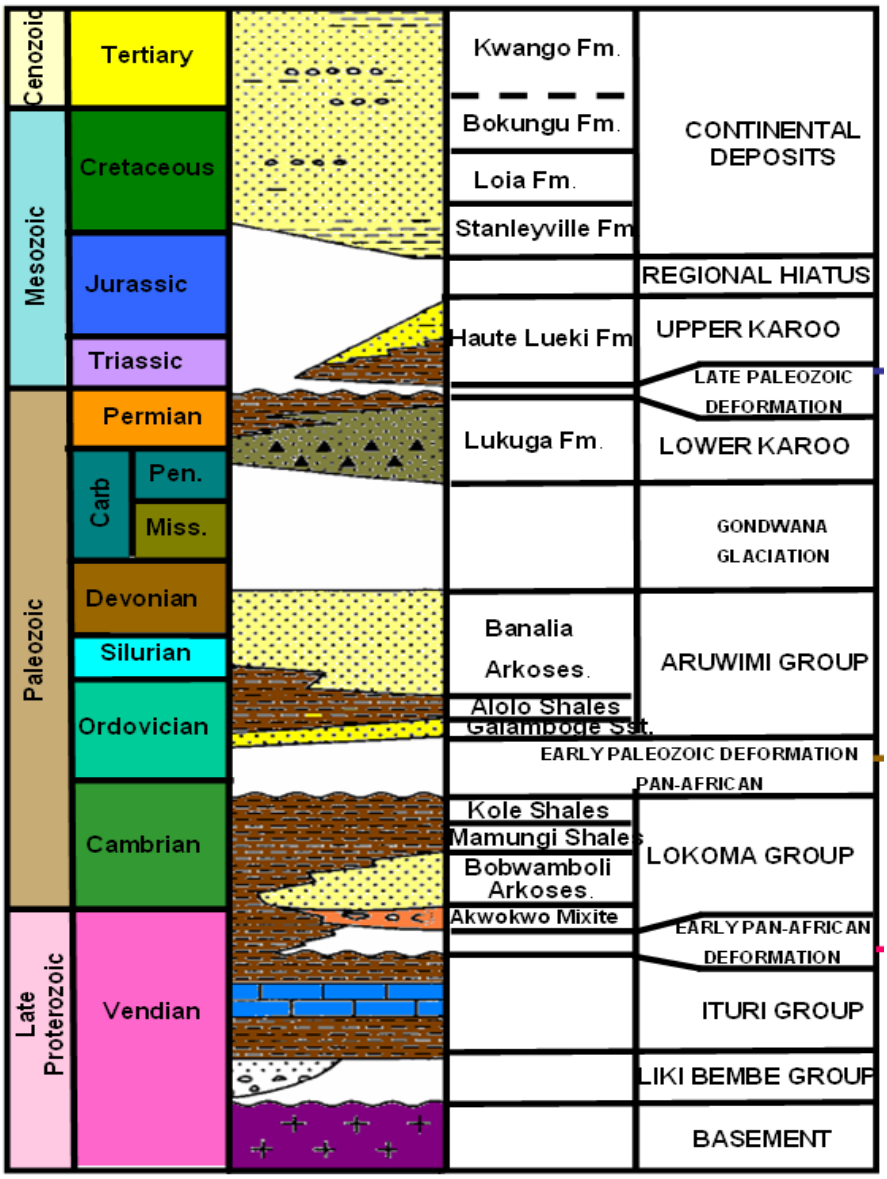

Figure 4. *Stratigraphy of Cuvette Centrale* [1].

DATA PROCESSING AND INTERPRETATION

Magnetic anomalies

Magnetic anomalies reflect variations in the distribution and type of magnetic iron oxide minerals, mainly magnetite, in the Earth's crust. Airborne magnetic data generally image the first 10 km of the crust, down to the crystalline basement of the areas studied.

Horizontal resolution depends on flight-line spacing and survey altitude, but varies from meter-scale to continental scale. On a regional scale, positive magnetic anomalies are often associated with magnetite-rich batholiths, large quantities of volcanic rocks and metamorphic rocks with igneous mafic protoliths. On a regional scale, negative magnetic anomalies (blue on magnetic maps) can be due to magnetite-poor sedimentary rocks, altered or magnetically reversed volcanic rocks, felsic plutons and metamorphic rocks with sedimentary protoliths [6].

The magnetic anomaly map (Figure 5) shows that towards the NE and part of the SW end, the magnetic anomaly intensity of the Total Field is light, and in the center, moving towards the W and SE, the magnetic anomaly is heavy and shows a few peaks. These anomalies show two directions, one NW-SE located in the N part and the other NE-SW located to the S.

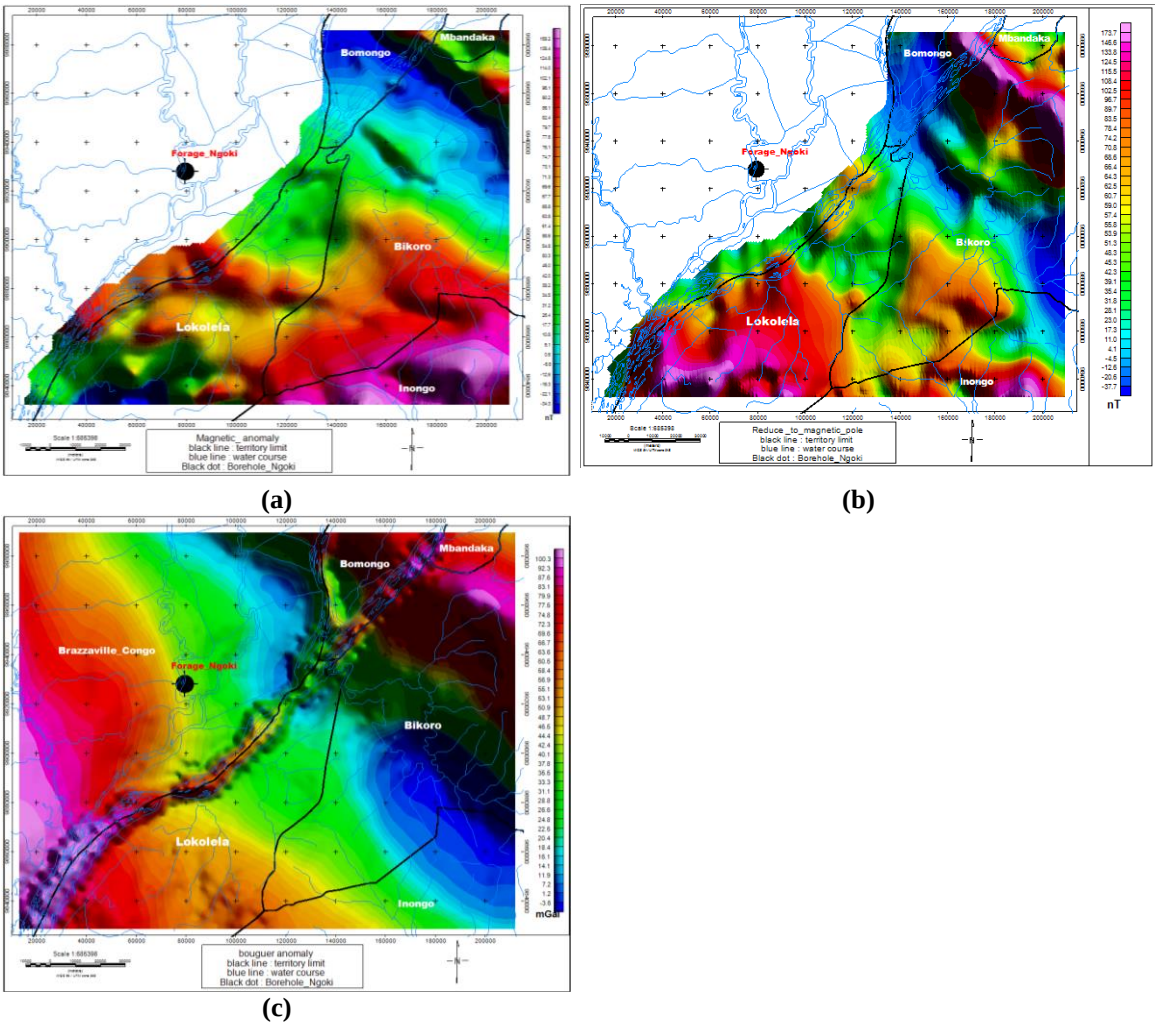

(a) **(b)**

(c)

***Figure 5**. Magnetic and gravimetric anomaly map (a: total field, b: pole reduction, and c: Bouguer anomaly).*

Reduction to pole

The first step is to reduce the magnetic data observed at the pole, a technique that takes into account the tilt of the Earth's magnetic field. Its main effect is to shift the magnetic anomalies directly above their source [7, 8]. The correction takes into account the effects of inclination and declination, assuming that the totality of the magnetization vectors of the various sources of the anomalies deviate by about 25 degrees from collinearity with the Earth's field (induced field, no remanent magnetism) (Bath, 1968). For the map of reduced magnetic anomalies at the pole, we observe large-intensity anomalies to the SW and SE, as well as to the NE. Light anomalies are found in the center, moving towards NW and SW. There are two directions on the anomaly map: N-S towards the S and NW-SE towards the NE of the study area.

Bouguer anomaly

Once all these corrections have been made, the acquired gravity values can be used to calculate the Bouguer anomaly, which is a function of all density variations below the topographic surface. The Bouguer anomaly AB is expressed as follows:

$$AB = gmes - gth + 0.3086h + (0.3086h - 0.0491\rho h) + \rho T \quad (1)$$

where: ρ is the Bouguer reduction density;

h – altitude of the measurement point;

T is the terrain correction for density ρ.

The first step in processing gravity data is to calculate the Bouguer anomaly, which is a function of all density variations below the topographic surface [9]. It represents the sum of contributions from geological bodies located at different depths, whose distribution is spread out from the surface to over 100 km.

To eliminate non-geological anomalies, measurements of "g" are compared with theoretical values of "g" on an "ideal" earth bounded no longer by the geoid but by the topographic surface. The Bouguer anomaly is defined as the anomaly between the measurement and the theoretical field at the measuring station The Bouguer anomaly is the gravimetric response caused by density heterogeneities in the subsurface. Interpretation is therefore based on the following formula:

$$\Delta gB = G\ observed \pm 5\ \text{corrections} \quad (2)$$

- Tide and instrument drift correction;
- Latitude correction $\Delta L = 8.1669 \times 10^{-4} \sin 2$ mGal;
- Altitude correction $\Delta h = 0.3086\ h$ mGal;
- Plateau correction $\Delta B = -0.04191$ mGal;
- Terrain correction ΔT and where h is in meters and is positive if the station is above the reference frame and negative if the station is below the reference frame:

$$\Delta G\ observed = G\ ob - g\ ref \quad (3)$$

It should be remembered that the measured gravity value is made on the earth's surface and not on the geoid. Therefore, the theoretical value is calculated in relation to the ellipsoid, which does not take into account the density of the various materials between the measurement surface and the reference surface. For measurements to be comparable, they all have to be brought back to the same reference plane, so a whole range of corrections is required [10, 11]. These various corrections lead to the definition of a set of values that characterize the so-called motion anomaly.

Indeed, the Bouguer anomaly map shown in the Figure 5 is the result of measured and theoretical gravity values, including all corrections. It shows slight anomalies in the center, moving north and SE. These are ellipsoidal in shape and oriented NW-SE. Heavy anomalies are found at the NE, SW and West ends. Along the Congo River, a heavy anomaly appears in the form of a NE-SW-trending vein. Heavy anomalies represent areas of shallower bedrock or high-density sedimentary rocks, while light anomalies indicate the presence of thick sedimentary rocks.

HORIZONTAL GRADIENT

In order to identify contacts that may represent faults, fractures or lithological boundaries, a function called maximum horizontal gradient is applied to airborne magnetic data, with peaks at contacts [8, 12, 13]. The transformation of magnetic data facilitates the interpretation of magnetic anomalies because the peaks of pseudogravity anomalies are directly centered on the contacts separating rocks of different magnetism, just as the horizontal gradients of gravity anomalies (Figure 6) are located on the contacts separating rocks of different density [8, 13].

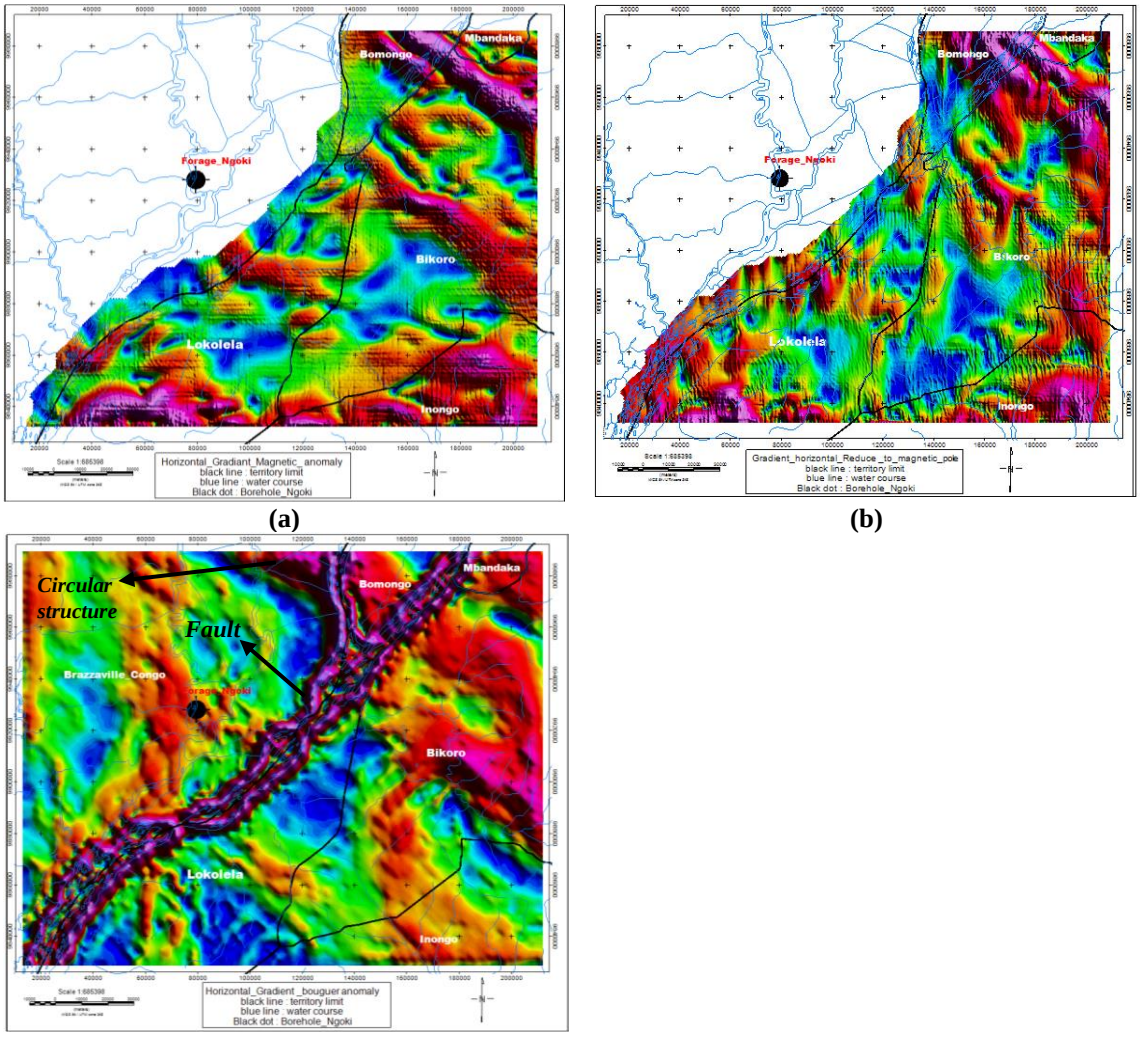

Figure 6. *Horizontal gradient map (a: total magnetic field anomalies. b: pole-reduced magnetic field anomalies, c: Bouguer anomalies).*

Magnetic anomaly

Two horizontal gradient and vertical derivative maps have been produced to highlight faulted geological structures or lithological contacts, in order to locate structures that may ensure hydrocarbon trapping.

Indeed, we note the presence of gradient maxima in both directional gradient maps, mostly NW-SE for total magnetic field anomalies and N-S for pole-reduced total magnetic field anomalies. Some directions, such as E-W, appear in the southern part of the horizontal gradient map (Figure 6), and NW-SE in the northern part of the horizontal gradient map for the pole-reduced magnetic field.

Bouguer anomaly

The Bouguer Anomaly Horizontal Gradient (Figure 6) shows a maximum anomaly oriented NE-SW along the Congo River. This maximum gradient represents the great fault on which the Congo River crosses as it flows SW. This great fault separates the Democratic Republic of Congo from the Republic of Congo. Linear structures are also observed, oriented NW-SE on the Democratic Republic of Congo side and N-S on the Republic of Congo side.

VERTICAL DERIVATIVES

The vertical derivative is used to better highlight surface anomalies by attenuating longer-wavelength (low-frequency) anomalies, and to locate the boundaries of structures [9].

Magnetic anomalies

The vertical derivative maps of the Total Magnetic Field anomalies and the Pole Reduced Magnetic Field anomalies show us a number of brittle structures, some of which are collapse faults, some of which are strike-slip faults.

As we can see from the Total Magnetic Field derivative map, along the Congo River, there is a large fault as previously visualized, which shifts the compartments in horizontal movement. On the Democratic Republic of Congo side, the fault is in dextral displacement, orienting the compartments to the NE, and on the Republic of Congo side, it is in sinister displacement, orienting the compartments to the SW (Figure 7a).

The map of the horizontal derivative of reduced magnetic anomalies at the pole shows collapse faults oriented N-S, most of which are located to the south, and the same type of faults to the north, but this time oriented NW-SE (Figure 7b).

Bouguer anomaly

Speaking of the Bouguer anomaly vertical derivative map, it presents the same information as the horizontal gradient map, where we observe the large NE-SW-trending fault. We thus observe circular structures that can give us information on the presence of anticlines (Figure 7c).

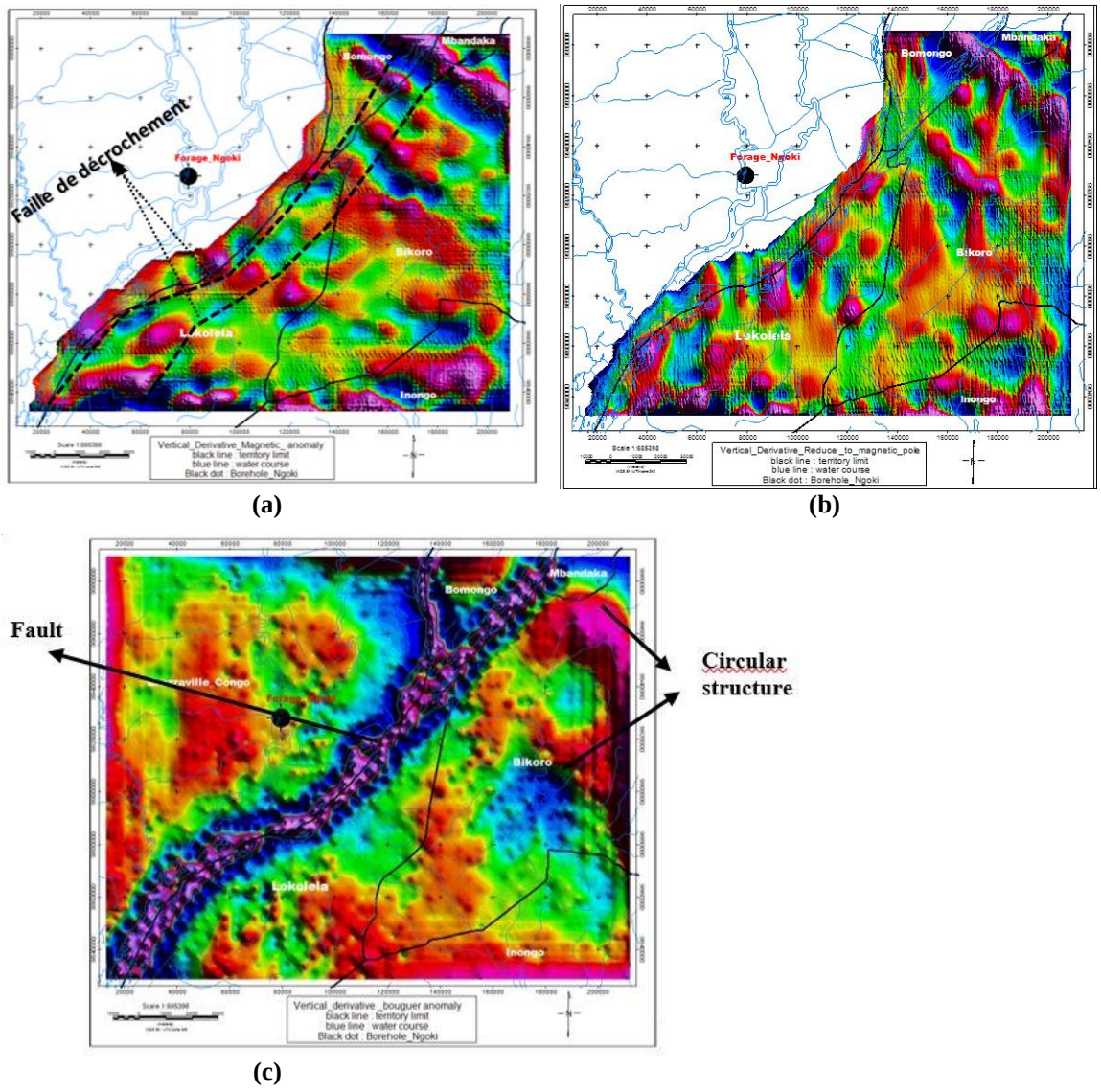

***Figure 7**. Vertical derivative map (a: total magnetic field anomalies, b: pole-reduced magnetic field anomalies, c: Bouguer anomalies)*

EULER DEPTH

The quality of Euler deconvolution evaluation depends largely on the appropriate choice of structural index (SI) [14, 15]. The method has been shown to be reasonably effective (compared with other depth evaluation algorithms) for determining the depth of magnetic sources, and particularly good for locating the horizontal position of such sources [15]. Extended Euler deconvolution represents a significant improvement over the standard method [16]. By employing the Euler homogeneity equation and assuming the uniqueness of the magnetic source, the vertical and horizontal gradients and Hilbert transforms of the measured magnetic field can be unambiguously related to the vertical and horizontal positions of the source [14, 17, 18].

A good clustering of solutions indicates that the source location is well resolved, and a scattering indicates that the solutions should probably be ignored [14]. The choice of source model, or structural index, is essential for reasonable results. The use of

inaccurate structural indices will lead to solutions that are widely dispersed and have imprecise depths. The structural index is directly related to the rate of decrease in field strength with distance from the magnetic source.

Geological structures have certain signatures that can be used to define source depths. These indices depend on the gravimetric and magnetic methods used. This filter is used to highlight geological structures such as Dykes, Sills, lithological contacts and faults. The configuration of these structures enables us to highlight anticlines, which are good traps for hydrocarbons. In the case of magnetic or gravimetric potential fields, the homogeneity condition is verified above all for simple geometries (sphere, contact, dyke) [14], i.e. for whole structural indices (0, 1, 2 and 3) (Table 1).

Table 1. *Determination of structural index according to source geometry for magnetism and gravimetry* [14].

Source	Gravity SI	Magnetism SI
Sphère	3	2
Cylindre	2	1
Dyke	1	0
Contact	0	-

Magnetic anomaly

Referring to the Euler depth map, we note that several circular lithological contacts are located in the northern and southern parts. The circular shape of these contacts or faults corresponds to anticlines, which are good traps for hydrocarbons. The faults on the contact depth map, deduced from Total Magnetic Field anomalies, show two orientations, one of which is NW-SE to the north, and NE-SW to the south (Figure 8a).

The map of contact depths from pole-reduced magnetic anomalies also shows circular contact shapes or faults that also correspond to anticlines. The same map shows two main fault or contact directions: NW-SE and NE-SW. NW-SW faults are found in the north, while NE-SW faults are found in the south (Figure 8b).

Bouguer anomaly

Interpretation of the map shown in Figure 8c has produced a structural map of the region showing the presence of anticlinoriums and faults. Faults in the region are predominantly NW-SE trending, some NNE-SSW. These faults ensure the migration of hydrocarbons, and anticlines are important geological structures for the accumulation of hydrocarbons. Based on the orientation of the faults, we note that hydrocarbon migration has followed a NW-SE path.

The great fault that subdivides the study area into two parts, oriented NE-SW, along which the Congo River flows, separating the two countries of DR Congo and the Republic of Congo, is a strike-slip fault. This fault shifts the anticlinal structures in two directions, NE and SW. The anticlines on the Democratic Republic of Congo side are offset to the NE with a Dextre drop-off, and on the Republic of Congo side, they are offset to the SW with a Senestre drop-off.

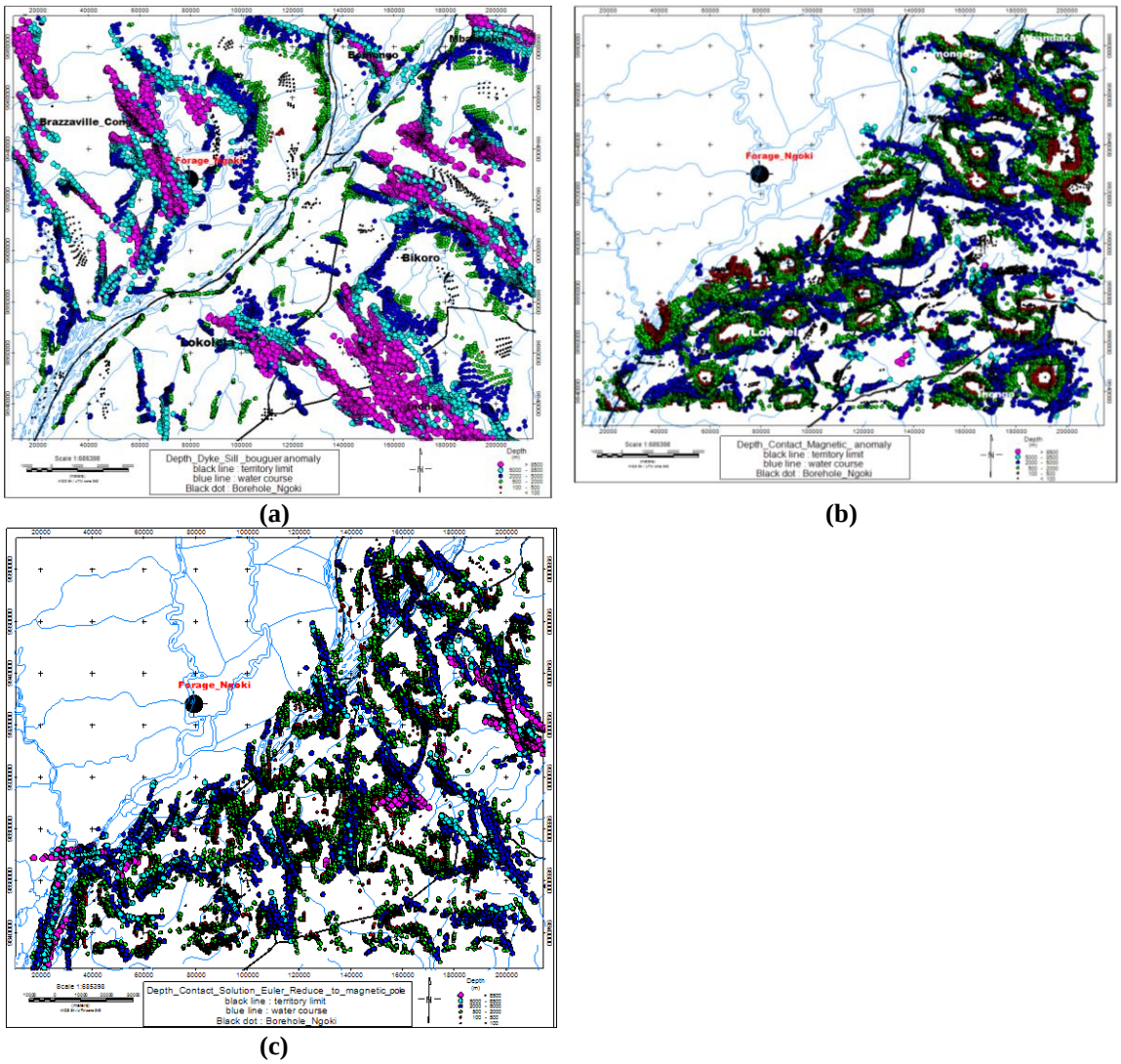

***Figure 8**. Euler solution (a: Gravimetry, SI=0 for Dykes and Sills; b: Total magnetic field, SI = 1 for contacts; c: Total reduced magnetic field, SI=0 for contacts)*

A structural map combining gravimetry and magnetometry was drawn up to understand the petroleum potential of this western part of the Democratic Republic of Congo. This western region of the Democratic Republic of Congo is potentially oil-rich, as it features geological structures such as faults, anticlines and faulted anticlines (Figure 9). The map shows anticlinal structures and faults of major petroleum interest as potential traps and migration routes for hydrocarbons.

CONCLUSIONS

The Central Basin is rich in oil potential. Several studies carried out in the Democratic Republic of Congo and the Republic of Congo have highlighted the geological structures, surface indications and elements of the petroleum system, including mature source rocks, reservoirs, covers and traps. Despite the presence of these highlighted elements linked to the petroleum system, four drillings carried out in the Central Cuvette Basin of DR Congo, none of them revealed a liter of oil on the surface.

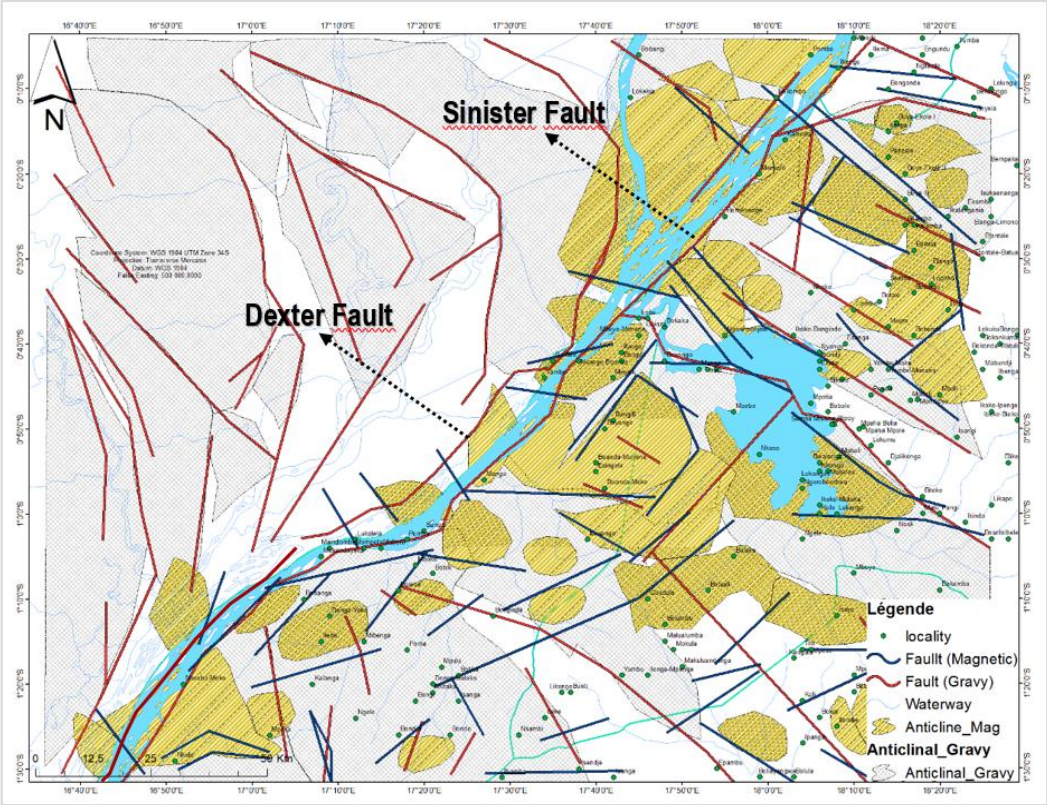

***Figure 9**. Structural map from Euler's solution*

In 2019, still in the Central Cuvette Basin of the Republic of Congo, precisely in the Ngoki block, one borehole drilled revealed the presence of profitable economic hydrocarbons. With a view to promoting the Cuvette Basin in DR Congo, we wanted to use this study to establish a structural correlation (geological structure of petroleum interest) between the western part of DR Congo and the Ngoki Block in the Republic of Congo.

To do this, we used gravity and magnetic data from geophysical exploration campaigns in DR Congo to highlight geological structures of petroleum interest. After processing and interpretation, we understand that the region contains interesting structures linked to hydrocarbon trapping. These include anticlines and faults. We discovered that there is a close relationship between the geological structures of these two countries (DR Congo and R Congo). They are all made up of the same geological structures, separated by two major strike-slip faults (Dextre and Senestre) where the Congo River flows (NE-SW direction), creating a displacement movement moving the compartment on the DR Congo side in the SW-NE direction and NE-SW on the R Congo side.

REFERENCES

[1] Secrétariat Général aux Hydrocarbures, Les Bassins sédimentaires de la RD Congo, Kinshasa, R.D. Congo. https://fr.scribd.com/document/515762415, 2011

[2] Site: www.lepatriote-congobrazza.com, Les concessions pétrolières menacent le deuxième poumon du monde dans la cuvette Centrale, Bassin du Congo | EJAtlas. www.lepatriote-congobrazza.com, 2022

[3] Lepersonne J., Carte géologique du Zaïre echelle 1/2.000.000 et Notice explicative - République du Zaïre, Département des Mines, Direction de la Géologie, Kinshasa, 1974

[4] CTP/Pétrozaire. Promotion de pétrole de la Cuvette Centrale/République du Zaïre (Rapport du projet). 1987

[5] SONAHYDROC, Certification des réserves des bassins sédimentaires de la République Démocratique du Congo. 2012

[6] Finn C.A., Anderson E.D., Synthèse des données géophysiques. Second Projet de Renforcement Institutionnel du Secteur Minier de la République Islamique de Mauritanie (PRISM-II), Phase V. https://pubs.usgs.gov/of/2013/1280, 2013

[7] Baranov V., Naudy H., Numerical calculation of the formula of reduction to the magnetic pole, Geophysics, v. 29, p. 67-79, 1964

[8] Blakely R.J., Simpson R.W., Short Note: Approximating edges of source bodies from magnetic or gravity anomalies, Geophysics, 51(7), 1494-1498, 1986

[9] Dubois J., Diament M., Cogne J-P., Géophysique (cours et exercices corrigés 4è édition). Ed. Dunod, Paris, 2011

[10] LaFehr T.R., Standardization in gravity reduction, Geophysics, 56 (8), 1170-1178, 1991

[11] Hackney R.I., Featherstone W.E., Geodetic versus geophysical perspectives of the 'gravity anomaly'. Geophysical Journal International, 154 (1), 35-43, 2003

[12] Cordell L., Grauch V.J.S., Mapping basement magnetization zones from aeromagnetic data in the San Juan basin, New Mexico: in Hinze W.J., Ed., The Utility of Regional Gravity and Magnetic Anomaly maps: Soc. Expl. Geophys., 181-197, 1985

[13] Grauch V.J.S., Cordell L., Short Note: Limitations of determining density or magnetic boundaries from the horizontal gradient of gravity or pseudogravity data, Geophysics, 52 (1), 118-121, 1987

[14] Thompson D.T., EULDPH: A new technique for making computer-assisted depth estimates from magnetic data: Geophysics, v. 47, p. 31-37, 1982

[15] Reid A.B., Allsop J.M., Granser H., Millett A.J., Somerton I.W., Magnetic interpretation in three dimensions using Euler deconvolution: Geophysics, 55 (1), 80-91, 1990

[16] Phillips J.D., Two-step processing for 3D magnetic source locations and structural indices using extended Euler or analytic signal methods, Society of Exploration Geophysicists, Technical Program Expanded Abstracts, v. 21, 727-730, 2002

[17] Mushayandebvu M.F., van Driel P., Reid A.B., Fairhead J.D., Magnetic source parameters of two-dimensional structures using extended Euler deconvolution, Geophysics, 66 (3), 814-823, 2001

[18] Nabighian M.N., Hansen, R.O., Unification of Euler and Werner deconvolution in three dimensions via the generalized Hilbert transform, Geophysics, 66 (6), 1805-1810, 2001

Received: October 2023; Revised: January 2024; Accepted: February 2024; Published: February 2024